Received 16 January 2024; revised 1 March 2024; accepted 9 March 2024. Date of publication 18 March 2024; date of current version 27 May 2024.

Digital Object Identifier 10.1109/OJAP.2024.3376568

A Single-Antenna Full-Duplex Subsystem With High Isolation and High Gain

LI ZHANG[1,2], MIAO LV[1,2], ZHI-YA ZHANG[1], YU WANG[2,3], FANCHAO ZENG[4] (Graduate Student Member, IEEE), CAN DING[4], AND CHENHUI DAI[1]

[1]National Key Laboratory of Science and Technology on Antennas and Microwaves, Xidian University, Xi'an 710071, China

[2]The 20th Research Institute of China Electronics Technology Corporation, Xi'an 710068, China

[3]CETC Key Laboratory of Data Link Technology, Xi'an 710068, China

[4]Global Big Data Technologies Centre, University of Technology Sydney, Sydney, NSW 2007, Australia

CORRESPONDING AUTHORS: Z.-Y. ZHANG AND F. ZENG (e-mail: zyzhang@xidian.edu.cn; Fanchao.zeng@student.uts.edu.au)

This work was supported in part by the National Natural Science Foundation of China under Grant 62271372; in part by the CETC Key Laboratory of Data Link Technology under Grant CLDL-20202413; and in part by NSFC.

ABSTRACT In this paper, a single-antenna full-duplex subsystem is proposed, consisting of a high isolation network and a stacked patch antenna with reflector. The employed patch antenna is fed by two ports with very similar input impedances to make the reflected signals identical. The high isolation network composed of two hybrids and two circulators plays a crucial part in achieving high transmitting to receiving (Tx-Rx) isolation. It is able to cancel out the inevitable reflected signals from the antenna ports and the leakage signals from the circulators. The theoretical analysis is presented and the subsystem is also fabricated and measured. According to the measurement results, across the operation band from 2.018 to 2.12 GHz, the subsystem has VSWR < 1.55, Tx-Rx isolation > 50 dB, axial ratio < 2.4, and gain > 10.2 dBic. Compared with the state-of-art single-antenna full-duplex subsystems, the proposed design features high Tx-Rx isolation level and high gain, which is suitable for microwave radio relay communication and satellite detection application.

INDEX TERMS Full-duplex, high isolation network, transmitting to receiving (Tx-Rx) isolation, reflector antenna.

I. INTRODUCTION

A FULL-DUPLEX system can transmit and receive signals simultaneously, which increases spectral efficiency and theoretically doubles data rate compared to traditional frequency or time division duplexing systems [1]. However, in practice, a full-duplex system is considered difficult to implement due to the potentially significant self-interference (SI) between the transmitting (Tx) and receiving (Rx) signals [2]. Efforts have been made to mitigate the SI of full-duplex systems in both the digital, analog, or antenna domains [3]. Specifically, if good isolation between the Tx and Rx signals can be obtained in the antenna domain, this can take some loads from the subsequent analog and digital TR module, thereby lowering the cost of the entire full-duplex system. There exist various approaches that can attain a high level of isolation between Tx and Rx antennas in full-duplex antenna subsystems, such as space separation [4], [5], [6], polarization diversity [7], [8], [9], [10], near-field cancellation [11], [12], [13], [14], and the utilization of circulator [15]. Although these techniques can achieve good isolation, they still require multiple Tx and Rx antennas, thus the subsystem is not ideal. Ideally, a full-duplex antenna subsystem should only use one antenna for both Tx and Rx purposes, namely, a single-antenna full-duplex subsystem.

The first single-antenna full-duplex subsystem was proposed in [16]. The system has a balanced feed network consisting of circulators and quadrature hybrids, which is able to cancel the antenna reflection and circulator leakage, thereby achieving a high Tx-Rx isolation of 40-45 dB across a narrow band of 902-928 MHz. Literatures [17], [18] utilized dual-polarized microstrip patch antennas and

180° ring hybrid couplers to achieve the full-duplex performance. Ultra-high interport isolation of 90 dB has been achieved but the bandwidth is also quite narrow, i.e., 20 MHz. Spiral antennas with multiple arms were used as the radiator in the full-duplex systems proposed in [19], [20]. Although different arms of the spirals are used for Tx and Rx, the arms are interleaved and considered as one antenna. These works have a very wide bandwidth, but the achieved isolation level is relatively lower, i.e., > 38 dB.

It should be noted that the aforementioned works all have limited gains less than 5 dBi/dBic. In some applications for microwave radio relay communication and satellite detection purposes, antenna gain, rather than the bandwidth, is the major concern. Because of the complexity of the feed networks in full-duplex systems, it is hard to expand the antennas proposed in [16], [17], [18], [19], [20] into arrays to attain higher gain. Instead, a high gain radiator should be incorporated in the full-duplex system. In [21], a reflector antenna with modified coaxial cavity antenna as feed and apex matching technology was demonstrated, which achieved a very high gain of 21 dBic. The full-duplex subsystem also has a wide bandwidth from 4 to 8 GHz. However, because of the amplitude and phase imbalances of the employed components, the system has a relatively lower Tx-Rx isolation level, i.e., > 30 dB. Several other works have been proposed to achieve high gain [22], [23], [24]. However, attaining high Tx-Rx isolation remains a challenging endeavor.

In this work, a single-antenna full-duplex subsystem with high Tx-Rx isolation and high gain is proposed. A dual-fed stacked patch antenna with reflector is employed as the radiator to achieve a high gain. An impedance matching network is used to achieve excellent match and makes the amplitude of the reflected signals equal. Additionally, a high isolation network is integral in this design, effectively cancelling undesired signals through equal amplitude and 180° phase difference, thereby achieving high Tx-Rx isolation. The proposed full-duplex subsystem is fabricated, measured, and compared with state-of-the-art designs. The comparison shows that the proposed full-duplex subsystem exhibits higher gain and higher isolation level across a reasonable wide bandwidth, which serves as an excellent candidate for microwave radio relay communication and satellite detection application.

The main contributions that we describe in this paper are as follow. What distinguishes our work from the aforementioned citations is, rather than typically focus on a single characteristic, for instance, gain, Tx-Rx isolation, or bandwidth. Our work takes a holistic approach, addressing all these aspects simultaneously to enhance the overall performance, making it more practical for real-world applications. And instead of using the antenna array with complex feeding and decoupling network, the proposed system feathers simple structure for a single-antenna full-duplex subsystem.

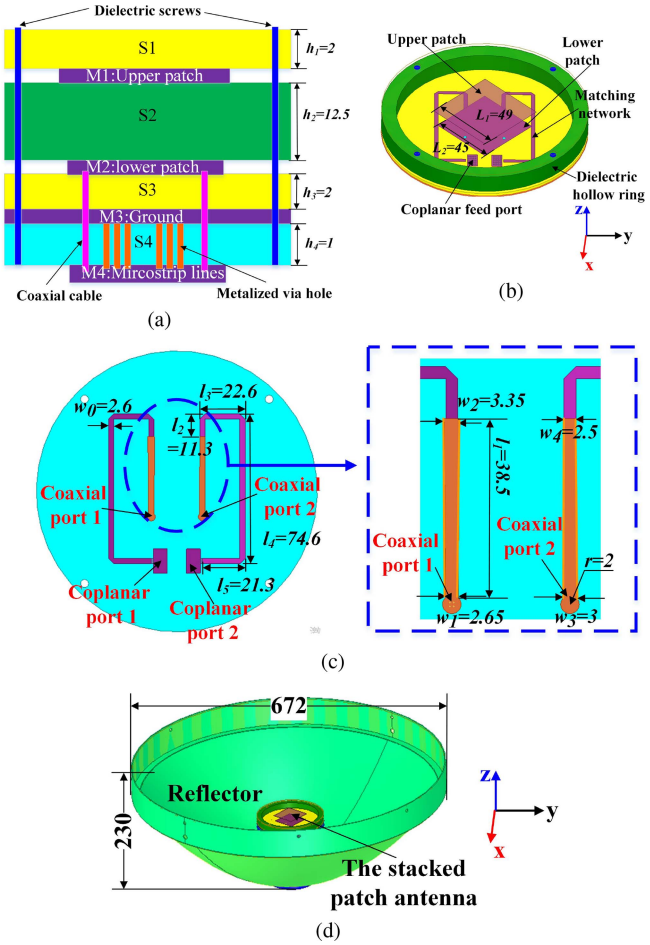

FIGURE 1. (a) Side view and (b) perspective view of the proposed antenna. (c) Detailed view of the impedance matching network on layer 4. (d) Perspective view of the antenna with reflector. (All the units are in mm.).

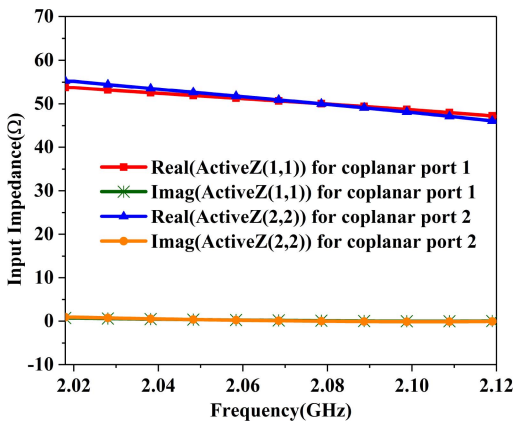

FIGURE 2. Simulated real and imaginary parts of the input impedance of the antenna at the two coplanar ports.

II. RADIATOR

The configuration of the proposed dual-fed CP antenna is shown in Fig. 1. The antenna consists of four substrate layers (S1-S4) and four metal layers (M1-M4), see Fig. 1(a). Layers S1, S3, and S4 have the same relative permittivity of 2.65

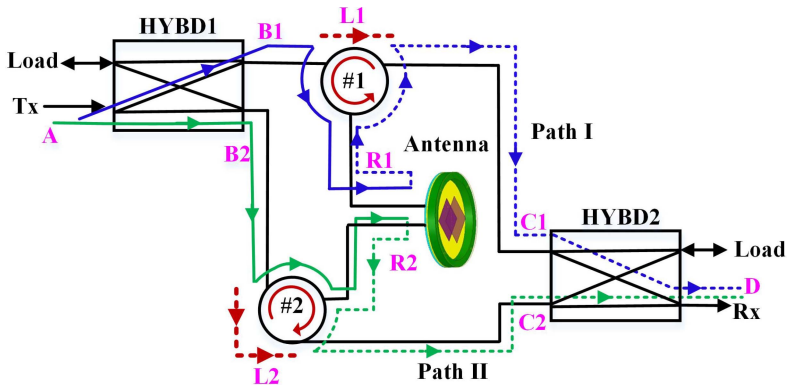

FIGURE 3. Schematic diagram of the proposed single-antenna full-duplex subsystem.

and a loss tangent of 0.001. Layer S2 is a dielectric hollow ring with the relative permittivity of 3.5 and loss tangent of 0.001. The thicknesses of the substrate layers are labelled in Fig. 1(a). The metal layers are all very thin (0.017 mm) and are printed on the substrates. There are four dielectric screws run through the four substrate layers to fix them together.

As shown in Figs. 1(a) and 1(b), two metal square patches (M1 and M2) form into a stacked patch, which is the main radiator. The lower patch is fed by two coaxial probes. To facilitate the connection between the antenna and the subsequent high isolation network, the two coaxial ports are transited to two coplanar feed ports through a pair of microstrip lines located on M4. The details of the microstrip-based transition structure are shown in Fig. 1(c). The coplanar port feathers a rectangular metal patch that is connect the ground through several metalized via holes. This design ensures that the metal ground and microstrip lines are one the same layer, which facilitates the process of soldering the coaxial cable. The patch on M2 and the microstrip lines on M4 share the same ground plane on M3. Moreover, a reflector shown in Fig. 1(d) is used to enhance the gain of the stacked patch antenna within the operation band.

The stacked patch antenna is employed as it has wider operational bandwidth compared to conventional single-layer ones. Utilizing both the upper and lower patches allows the antenna to create two resonance points, leading to a stable impedance. This design significantly extends the bandwidth of the stacked patch antenna. The stable impedance and wider bandwidth of the antenna facilitate easier matching with the feeding network, ensuring consistent high isolation, even when the circulator's impedance varies. By tuning the dimensions of the microstrip-based transition structure as shown in Fig. 1(c), the real and imaginary parts of the input impedances at the two coplanar ports can be tuned to 50 Ω and 0 Ω, respectively, as shown in Fig. 2. The difference of the input impedances between the two ports is less than 0.5 Ω. Hence, the amplitudes of the reflected signals from the two different ports of the antenna are prone to be equal.

III. HIGH ISOLATION NETWORK

Fig. 3 illustrates the signal flow diagram of the proposed full-duplex subsystem composed of a high isolation network and a stacked patch antenna. The isolation network consists of two hybrids and two circulators. Each quadrature hybrid provides an equal power split and 90° relative phase difference. The circulators rout a signal from the transmitter to the antenna and simultaneously rout a signal from the antenna to the receiver, but prevent the Tx signal from going into the Rx port directly.

The signal flow is illustrated using blue and green solid arrows in Fig. 3. First, the Tx signal A splits into two signals, B1 and B2, after going through the first hybrid. The resultant two signals have the same amplitude and a phase shift of 90°, i.e., B2 = B1e-j90°. Then the two signals are directed to the two ports of the antennas through two circulators, leading to CP radiation.

Ideally, the Tx and Rx ports are well isolated. However, in reality, the Tx signal can enter the Rx port due to the following two reasons. First, the employed circulators are not ideal and can have some leakages (L1 and L2), as illustrated by red dashed arrows in Fig. 3. Second, due to the antenna mismatch, a small portion of the input power of the Tx signal is reflected back (R1 and R2). Two paths of the reflected signal flow are illustrated in Fig. 3 using green and blue dashed arrows. All the reflected signals and the leakage signals will add together into D after the second hybrid and enter the Rx port. Nevertheless, the proposed subsystem can still exhibit a high isolation level, because the leakage signals and the reflected signals can be cancelled out at the Rx port. In specific,

$$\begin{aligned} D &= C1e^{j90^\circ} + C2 \\ &= (L1 + R1)\ e^{j90^\circ} + (L2 + R2) \end{aligned} \tag{1}$$

and

$$L1 = \alpha_1 B_1, R1 = \beta_1 B1, L2 = \alpha_2 B2, R2 = \beta_2 B2 \tag{2}$$

where $\alpha 1$ and $\alpha 2$ represent the leakage rates of the two circulators; $\beta 1$ and $\beta 2$ represent the reflected ratios at the two antenna ports. Considering the symmetry of the structure and we use the same circulators,

$$\alpha_1 \approx \alpha_2, \beta_1 \approx \beta_2 \tag{3}$$

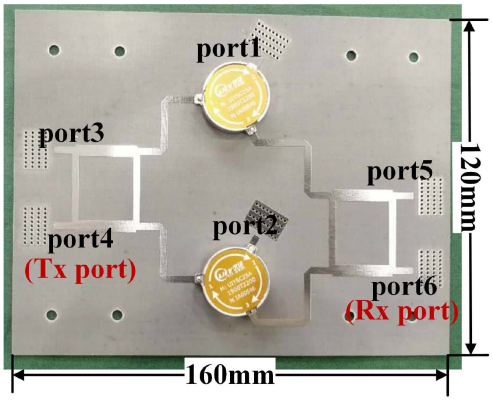

FIGURE 4. Fabricated prototype of the high isolation network.

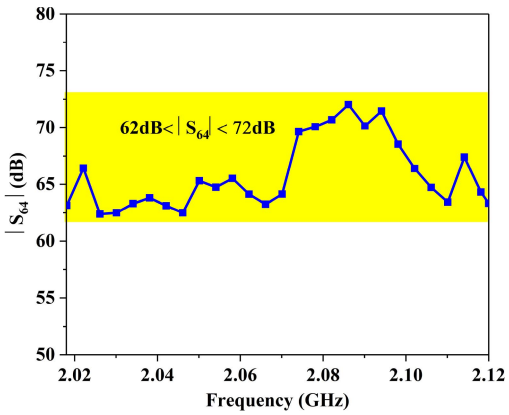

FIGURE 5. Simulated Tx-Rx isolation, i.e., $|S_{64}|$ of the high isolation network, with ports 1 and 2 connected with 50 Ω load.

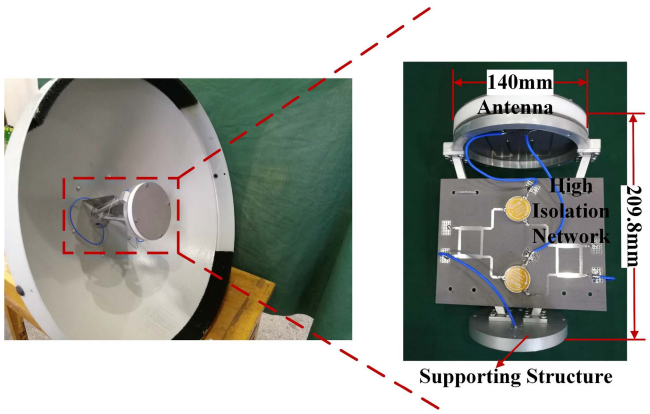

FIGURE 6. Fabricated prototype of the proposed antenna subsystem.

Also, since $\mathbf{B2} = \mathbf{B}1e^{-j90^\circ}$, then we have

$$\begin{aligned} D &= (\alpha_1 B_1 + \beta_1 B1)e^{j90^\circ} + (\alpha_1 B_1 + \beta_1 B1)e^{-j90^\circ} \\ &= j(\alpha_1 B_1 + \beta_1 B1) - j(\alpha_1 B_1 + \beta_1 B1) \\ &= 0. \end{aligned} \tag{4}$$

Thus, it can be concluded that, despite the inevitable limitations of the circulator leakage and the antenna mismatch, the resultant imbalances can be cancelled out, which leads

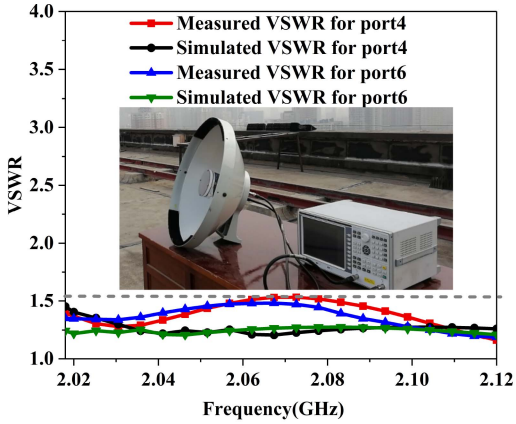

(a)

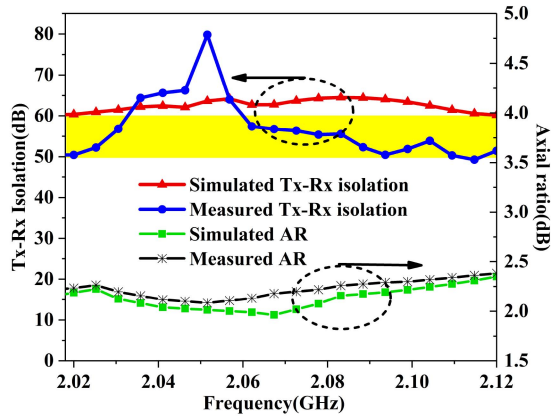

(b)

FIGURE 7. Simulated and measured (a) VSWR at the Tx and Rx ports; (b) Tx-Rx isolation and AR.

to a high Tx-Rx isolation level. The fabricated high isolation network is illustrated in Fig. 4. The microstrip quadrature hybrid is printed on the top side of a 1-mm-thick substrate with a relative permittivity of 2.65 and a loss tangent of 0.001. Two surface-mount circulators [25] with isolation of 23 dB and low insertion loss of 0.3 dB are fixed on the top surface of the substrate plane using surface mount technology (SMT).

To assess the performance of the high isolation network, a simulation was conducted in Ansys HFSS considering the imperfectness of the hybrids and circulators. The circulators were modelled according to the datasheet [25]. Ports 1 and 2 are connected to a 50 Ω load to eliminate the effects of the antenna. The simulated isolation level between the Tx and Rx ports, i.e., ports 4 and 6, is plotted in Fig. 5. According to the simulation results, the proposed high isolation network provides a high Tx-Rx isolation > 62 dB across the target frequency band.

IV. MEASUREMENT RESULTS

The prototype of the entire single-antenna full-duplex subsystem was also fabricated and tested. The prototype is shown in Fig. 6. The dual-fed stacked patch antenna and

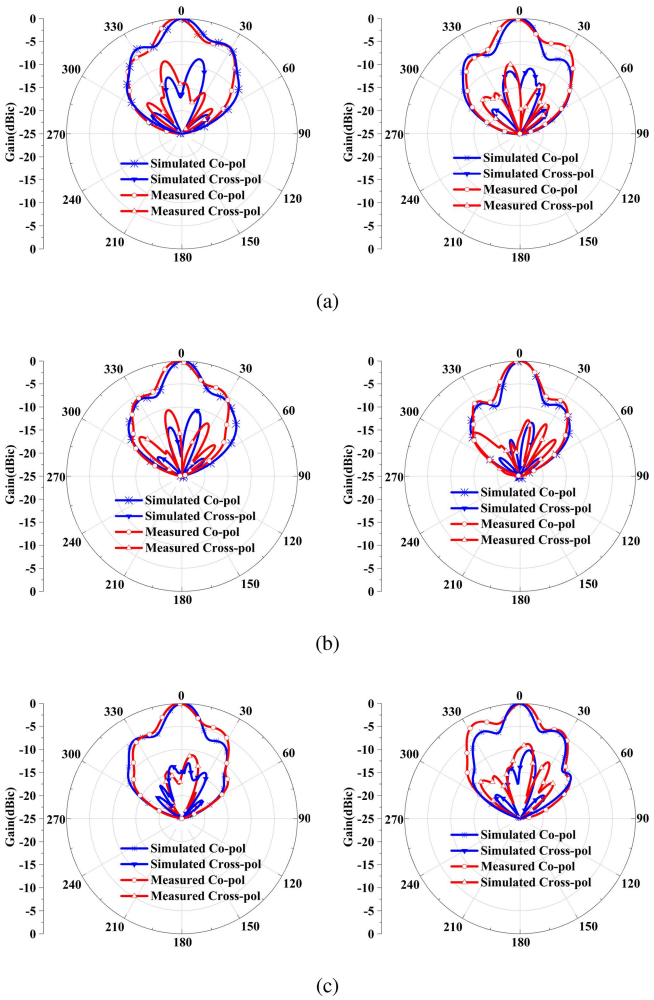

FIGURE 8. Simulated and measured co-pol (RHCP) and cross-pol (LHCP) radiation patterns in the x-z (left subplots) and y-z plane (right subplots) at (a) 2.018 GHz, (b) 2.069 GHz, and (c) 2.12 GHz.

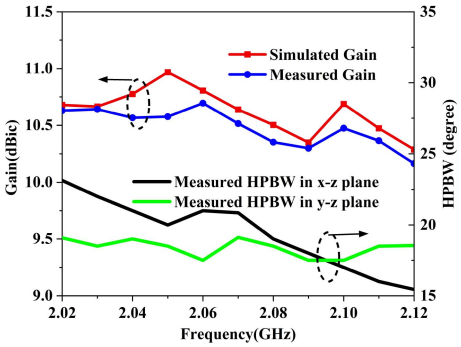

FIGURE 9. Simulated and measured realized gain and HPBW of the antenna subsystem at the Tx port.

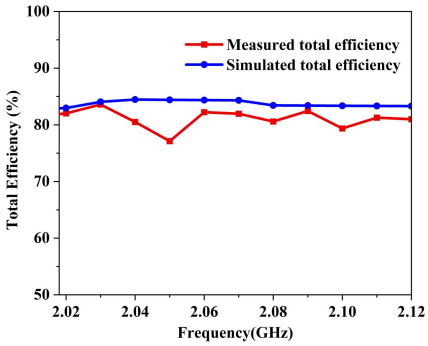

FIGURE 10. Measured and simulated total efficiency of the proposed antenna system.

the high isolation network are fixed together by a dielectric supporting structure and mounted on the reflector. The two ports of the patch antenna are connected with Port 1 and Port 2 of the high isolation network, respectively, using two subminiature version A (SMA) semirigid cables. The proposed antenna subsystem was measured by an Agilent E8363B network analyzer and a SATIMO far-field measurement system.

Fig. 7(a) shows the simulated and measure VSWRs at the Tx and Rx ports. The simulated and measured axial ratio (AR) at the Tx and Rx ports and the isolation between the two ports are plotted in Fig. 7(b). The simulated and measured results generally agree quite well. The small discrepancies are attributed to the imperfections of the fabrication and assembling of the antenna and the phase differences of the two cables. For the measurement results, across the operation frequency band from 2.018 to 2.12 GHz, the VSWRs for the two ports are < 1.55; the ARs for the two ports are < 2.4 dB; the Tx-Rx isolation is $>$ 50 dB. The normalized radiation patterns at three sample frequencies are shown in Figs. 8(a) to 8(c). Fig. 9 illustrates the realized gain and Half-Power Beamwidth (HPBW) across the entire frequency band. The measurement results indicate a consistently high gain, exceeding 10.2 dBic, along with stable radiation patterns throughout the band. Specifically, the HPBW remains approximately 19° in the y-z plane, while in the x-z plane, it varies between 15° and 23°. Fig. 10 presents the measured and simulated total efficiency of the proposed antenna system. Throughout the operating band, the radiation efficiency is over 75%, indicating high performance of the antenna.

To demonstrate the superiority of this work, the proposed single antenna full-duplex subsystem is compared with state-of-the-art works in Table 1. On one hand, the achieved gain in this work is 10.2 dBic, which is higher than all the other works except [21]. Although [21] has a very high gain, the Tx-Rx isolation level is only $>$ 30 dB. On the other hand, the proposed full-duplex antenna subsystem has a high Tx-Rx isolation level of $>$ 50 dB, which is higher than all the other works based on single polarization antenna subsystem. References [17], [18] achieved higher isolation because they used one polarization for transmitting and the other orthogonal polarization for receiving. If additional polarization diversity technique is implemented in this work, higher isolation level could also be achieved. Overall, it can be concluded that, the proposed single antenna full-duplex subsystem in this work achieves high

TABLE 1. Comparison between the state-of-art single-antenna full-duplex subsystems.

Reference	Frequency (GHz)	SIC (dB)	Polarization	Gain (dB/dBic)
[16]	0.902-0.928	40-45	Single CP	N.A.
[17]	2.4 (<50 MHz)	60-80	Dual LP	> 4.1
[18]	2.4 (20/40 MHz)	90/80	Dual LP	> 4
[19]	0.5-3.5	>37	Single CP	< 5
[20]	2-8	23-38	Single CP	> 3.8
[21]	4-8	>30	Single CP	> 20
This work	2.018-2.12	>50	Single CP	> 10.2

Tx-Rx isolation and high gain using simple method, thereby serving as an excellent candidate for microwave radio relay communication and satellite detection application.

V. CONCLUSION

A single-antenna full-duplex antenna subsystem with high gain and high Tx-Rx isolation level is designed for microwave radio relay communication and satellite detection purposes. The subsystem consists of a dual-fed stacked patch antenna connected by a high isolation network. The compact isolation network features low complexity but can intrinsically cancel out imperfections of the antenna and other employed components in the network, thus leads to a high Tx-Rx isolation. The working mechanism of the subsystem is discussed and then verified by simulations and measurements. The simulated and measured results agree very well with each other. Very good performances are attained according to the measurement results. At last, the proposed subsystem is further compared with the state-of-art works to illustrate its superiority.

REFERENCES

[1] M. Heino, S. N. Venkatasubramanian, C. Icheln, and K. Haneda, "Design of wavetraps for isolation improvement in compact in-band full-duplex relay antennas," *IEEE Trans. Antennas Propag.*, vol. 64, no. 3, pp. 1061–1070, Mar. 2016.

[2] X. Quan, W. Pan, Z. Li, Y. Liu, and Y. Tang, "Hybrid SI cancellation for single-antenna full-duplex radios," *Electron. Lett.*, vol. 53, no. 24, pp. 1615–1617.

[3] H. Krishnaswamy et al., "Full-duplex in a hand-held device—From fundamental physics to complex integrated circuits, systems and networks: An overview of the Columbia FlexICoN project," in *Proc. 50th Asilomar Conf. Signals, Syst. Comput.*, 2016, pp. 1563–1567.

[4] M. Duarte and A. Sabharwal, "Full-duplex wireless communications using off-the-shelf radios: Feasibility and first results," in *Proc. Conf. Rec. 44th Asilomar Conf. Signals, Syst. Comput.*, 2010, pp. 1558–1562.

[5] J. I. Choi, M. Jain, K. Srinivasan, P. Levis, and S. Katti, "Achieving single channel, full duplex wireless communication," in *Proc. 16th Annu. Int. Conf. Mobile Comput. Netw.*, 2010, pp. 1–12. [Online]. Available: https://doi.org/10.1145/1859995.1859997

[6] E. Everett, A. Sahai, and A. Sabharwal, "Passive self-interference suppression for full-duplex infrastructure nodes," *IEEE Trans. Wireless Commun.*, vol. 13, no. 2, pp. 680–694, Feb. 2014.

[7] C.-Y.-D. Sim, C.-C. Chang, and J.-S. Row, "Dual-feed dual-polarized patch antenna with low cross polarization and high isolation," *IEEE Trans. Antennas Propag.*, vol. 57, no. 10, pp. 3321–3324, Oct. 2009.

[8] R. S. Hao, Y. J. Cheng, Y. F. Wu, and Y. Fan, "A W-band low-profile dual-polarized reflectarray with integrated feed for in-band full-duplex application," *IEEE Trans. Antennas Propag.*, vol. 69, no. 11, pp. 7222–7230, Nov. 2021.

[9] Y.-M. Zhang and J.-L. Li, "Differential-series-fed dual-polarized traveling-wave array for full-duplex applications," *IEEE Trans. Antennas Propag.*, vol. 68, no. 5, pp. 4097–4102, May 2020.

[10] Y.-M. Zhang, S. Zhang, J.-L. Li, and G. F. Pedersen, "A dual-Polarized linear antenna array with improved isolation using a slotline-based 180° hybrid for full-duplex applications," *IEEE Antennas Wireless Propag. Lett.*, vol. 18, pp. 348–352, 2019.

[11] J. Wu, M. Li, and N. Behdad, "A Wideband, unidirectional circularly polarized antenna for full-duplex applications," *IEEE Trans. Antennas Propag.*, vol. 66, no. 3, pp. 1559–1563, Mar. 2018.

[12] L. Sun, Y. Li, Z. Zhang, and Z. Feng, "Compact co-horizontally polarized full-duplex antenna with omnidirectional patterns," *IEEE Antennas Wireless Propag. Lett.*, vol. 18, pp. 1154–1158, 2019.

[13] R. Lian, T.-Y. Shih, Y. Yin, and N. Behdad, "A high-isolation, ultra-wideband simultaneous transmit and receive antenna with monopole-like radiation characteristics," *IEEE Trans. Antennas Propag.*, vol. 66, no. 2, pp. 1002–1007, Feb. 2018.

[14] K. Kolodziej and B. Perry, "Vehicle-mounted STAR antenna isolation performance," in *Proc. IEEE Int. Symp. Antennas Propagat. USNC/URSI Nat. Radio Sci. Meet.*, 2015, pp. 1602–1603.

[15] J. L. Young, R. S. Adams, B. O'Neil, and C. M. Johnson, "Bandwidth optimization of an integrated microstrip circulator and antenna assembly. 1," *IEEE Antennas Propag. Mag.*, vol. 48, pp. 47–56, 2006.

[16] M. E. Knox, "Single antenna full duplex communications using a common carrier," in *Proc. IEEE Wireless Microw. Technol. Conf.*, 2012, pp. 1–6.

[17] H. Nawaz and I. Tekin, "Dual-polarized, differential fed microstrip patch antennas with very high interport isolation for full-duplex communication," *IEEE Trans. Antennas Propag.*, vol. 65, no. 12, pp. 7355–7360, Dec. 2017.

[18] H. Nawaz and I. Tekin, "Double-differential-fed, dual-polarized patch antenna with 90 dB interport RF isolation for a 2.4 GHz in-band full-duplex transceiver," *IEEE Antennas Wireless Propag. Lett.*, vol. 17, pp. 287–290, 2018.

[19] E. A. Etellisi, M. A. Elmansouri, and D. S. Filipovic, "Wideband monostatic simultaneous transmit and receive (STAR) antenna," *IEEE Trans. Antennas Propag.*, vol. 64, no. 1, pp. 6–15, Jan. 2016.

[20] E. A. Etellisi, M. A. Elmansouri, and D. S. Filipović, "Wideband multimode monostatic spiral antenna STAR subsystem," *IEEE Trans. Antennas Propag.*, vol. 65, no. 4, pp. 1845–1854, Apr. 2017.

[21] P. V. Prasannakumar, M. A. Elmansouri, and D. S. Filipovic, "Broadband reflector antenna with high isolation feed for full-duplex applications," *IEEE Trans. Antennas Propag.*, vol. 66, no. 5, pp. 2281–2290, May 2018.

[22] Y.-H. Huang, Q. Wu, and Q.-Z. Liu, "Broadband dual-polarised antenna with high isolation for wireless communication," *Electron. Lett.*, vol. 45, no. 14, pp. 714–715, 2009.

[23] B. Li, Y.-Z. Yin, W. Hu, Y. Ding, and Y. Zhao, "Wideband dual-polarized patch antenna with low cross polarization and high isolation," *IEEE Antennas Wireless Propag. Lett.*, vol. 11, pp. 427–430, 2012.

[24] S.-G. Zhou, G.-L. Huang, T.-H. Chio, J.-J. Yang, and G. Wei, "Design of a wideband dual-polarization full-corporate waveguide feed antenna array," *IEEE Trans. antennas Propag.*, vol. 63, no. 11, pp. 4775–4782, Nov. 2015.

[25] "200 to 3600MHz—Surface mount circulator," Datasheet, UIY Inc., Shenzhen, China, Mar. 2020. [Online]. Available: https://www.uiy.com/Datasheet/UIYSC25A.pdf